Non-850nm Vertical Cavity Laser Applications and Manufacturing Technology

Klein Johnson, William Hogan, Matthew Dummer, and Mary Hibbs-Brenner

Vixar, Inc.
2950 Xenium Lane, Suite 104, Plymouth, MN 55441
Phone: (763) 746-8045 Email: wcampbell@vixarinc.com

Keywords: VCSEL, Laser, Plastic Fiber, Neural Stimulation, Atomic Clock

Abstract

This work will detail some of the efforts at Vixar to address several opportunities for Vertical-Cavity Surface-Emitting Lasers outside of traditional 850nm data communications markets, namely:

1) High temperature and high reliability AlGaInP-based 680nm VCSELs for sensor, biomedical, and plastic fiber applications,

2) Polarization stable AlGaAs-based 795nm VCSELs for atomic frequency references, and

3) InP-based strained InGaAs 1860nm VCSELs for neural stimulation, where we have achieved better than 7mW CW optical power at room temperature in a dielectric mirror VCSEL with a buried tunnel junction.

In addition to design and performance particulars covered here, in the talk we will emphasize some of the processing challenges unique to each wavelength range including epitaxial growth, non-epitaxial dielectric mirrors, and lateral oxidation of 4" wafer substrates. Other topics include reliability, wafer-level test, and precision die placement in chip-on-board packaging.

INTRODUCTION

Vertical-Cavity Surface-Emitting Lasers (VCSELs) emitting at 850nm based upon the AlGaAs material system have been the standard optical source for glass fiber-optic based data communication links since the mid-1990s, and have also found widespread use in optical computer mice. Together, these two applications make up the vast majority of VCSEL based products shipped to date. There do, however, exist other compelling opportunities for VCSELs operating outside this wavelength range that have yet to be commercialized.

APPLICATIONS

Plastic Optical Fiber (POF) is beginning to be considered for home networks and consumer data links such as HDMI, Display-Port, and Thunderbolt. Data rates of these inter-connects have been increasing rapidly, to speeds of multi giga-bits per second that cannot be achieved by conventional LEDs or resonant cavity LEDs emitting around 650nm where the fiber loss is acceptable. (Fig. 1) Edge-emitting lasers suffer from high power consumption and a lack of compatibility with low-cost chip on board or surface mount packaging options.

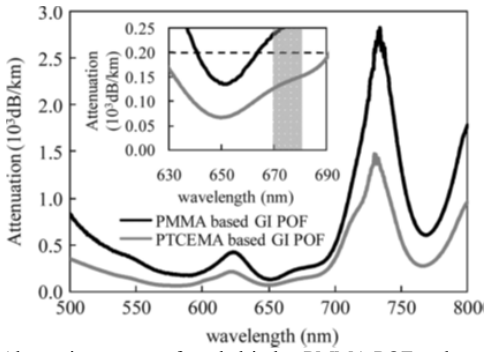

Figure 1 Absorption curves of graded-index PMMA POF and partially chlorinated plastic optical fiber. [1]

Interest in high speed visible VCSELs for POF is driven in part by recent enhancements made to fiber performance beyond that available from standard 1mm diameter step index PMMA. Graded index large core POF increases the fiber bandwidth significantly, requiring high speed sources to take advantage of these gains [2]. Partially chlorinated POF reduces the loss in the 660-685nm wavelength range [3], making 680nm VCSELs an attractive solution.

Visible VCSELs may also find use in a number of emerging biomedical applications. Light therapy is the use of low levels of visible or near infrared light to stimulate cell growth, reduce pain and inflammation, and accelerate wound healing [4]. Non-invasive optically based medical sensors for pulse oximetry, and the emerging application of tissue oximetry take advantage of the varying absorption coefficients of the different types of hemoglobin in the regime from about 660nm to 1000nm to measure their concentration in the blood [5]. These applications may benefit from the narrow spectral linewidth and the slow spectral shift with temperature of VCSELs, while wireless

implementations benefit from their reduced power consumption as compared to LEDs.

VCSELs emitting at 795nm and 895nm are being explored as sources in atomic clocks, where there is a desire to incorporate small, low-cost, high-precision frequency references in communication networks and portable GPS receivers. Clocks based on Coherent Population Trapping (CPT) in Rubidium and Cesium atomic vapors have been shown to meet many of these requirements, at a fraction of the size and power of the quartz crystal oscillators currently in use [6]. The performance requirements for VCSELs in atomic clocks run to the extreme [7]. The lasers must emit in a wavelength that is exactly resonant with the optical transition wavelengths of 894.6nm or 794.8nm for Cesium or Rubidium respectively. In addition, the VCSEL must operate in a single stable linear polarization with a linewidth < 100MHz, and do so over the life of the clock.

Infrared neural stimulation (INS) is a new field of research that uses low power infrared light to excite neural tissue [8]. INS has several advantages over traditional electrical stimulation methods including improved spatial specificity, a larger difference between the stimulation and damage thresholds, and the lack of stimulation artifacts following neural response [8,9]. Wavelengths of 1840-1880nm are of interest because the steep increase in the absorption coefficient of tissue in this range allows the optical penetration depth to be specifically tailored for many neurologic applications [10]. The development of a compact implantable optical source is a critical step toward making INS a clinically useful technology. VCSELs are an attractive solution due to their small size, simple packaging geometry, and potential for high efficiency at low power [11].

680NM VISIBLE VCSELS

A cross-section of our typical oxide-isolated VCSEL structure is shown in Figure 2. The device consists of a substrate on which is grown n-type and p-type distributed Bragg reflectors (DBRs), between which is located a 1-λ resonant cavity containing 3 to 5 un-doped quantum wells and associated barriers. An optical and electrical aperture is formed at the center of the device by etching an annular mesa into the structure and laterally oxidizing a 30nm thick layer of 98% aluminum AlGaAs in saturated steam at 400-450C. A deep, multi-step proton implant electrically isolates adjacent devices and reduces bondpad capacitance. Prior to evaporating the thick Ti/Au contact ohmic/interconnect metallization, the etched features are planarized with BCB to facilitate metal step coverage. The substrate is thinned to ~150um before the depositing NiGeAu backside contact metal.

VCSELs in the 650–700nm emission wavelength range require the use of GaInP quantum wells with AlGaInP barrier layers nearly lattice matched to a GaAs substrate. Accordingly, several limitations exist: The available conduction band offset is small and ranges from approximately 0.17eV at 650nm to 0.23eV at 700nm. Therefore, thermal carrier overflow limits the maximum temperature of operation and peak power [12].

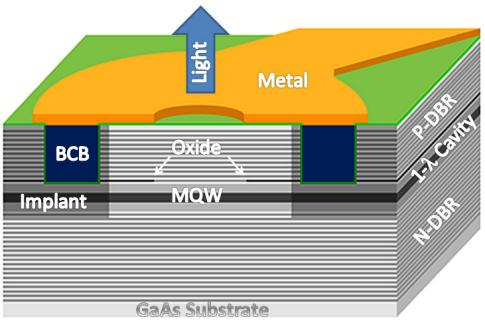

Figure 2 Cross-section of a typical oxide VCSEL structure.

The requirement that the AlGaAs mirrors be non-absorbing requires Al mole fractions greater than ~50%. This reduces the available range of refractive indices, requiring a large number of mirror periods to reach the 99.9% reflectivity required. Furthermore, the 50% AlGaAs composition has a higher thermal and electrical resistivity than compositions closer to the binaries. This results in both a higher conversion of input power to heat and more difficulty in removing this heat from the device, resulting in high junction temperatures and low optical power.

In our case, the crystal structure is grown on off-axis 4" n+ GaAs substrates using MOCVD. The mirror layers consist of 50% and 90% AlGaAs doped between 1e18 and 5e18 (carbon/silicon) with linearly graded interfaces. The bottom mirror consists of ~50 periods, and the number of top mirror periods is ~30. The active region consists of 3 compressively strained 6nm GaInP quantum wells with 6nm tensile strained AlGaInP barriers and a graded (50–70%) AlGaInP SCH. The p-side of the SCH is doped with Zn. A highly doped contact layer is grown at the top surface to facilitate formation of ohmic contacts. The oxide confinement layer is located 2 periods above the quantum well active region.

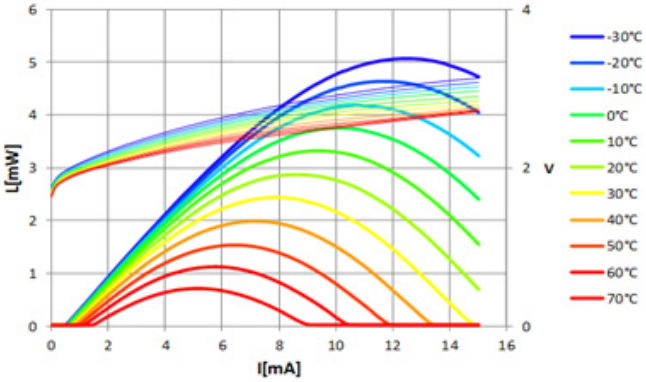

Figure 3 Performance curves over temperature for a 10um aperture 680nm VCSEL.

Careful optimization of the structure has enabled us to demonstrate very good performance characteristics. Figure 3 shows typical optical power and voltage performance for a 10um aperture 680nm device suitable for POF applications. This diameter device was chosen as to yield the best compromise in power, reliability, and temperature performance. Room temperature threshold currents are around 1mA. The expected drive current under use conditions is 3mA, so we anticipate a maximum operational temperature of 70C to be reasonable. High-speed performance is quite good as can be seen in Figure 4, which shows a 3Gb/s NRZ eye diagram taken at 70C with an extinction ratio of 8.5dB.

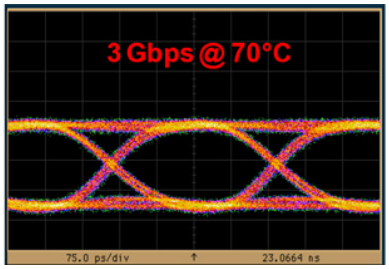

Figure 4 Eye diagram of 10um aperture 680nm VCSEL taken at 70C. Data rate is 3Gb/s and extinction ratio is >8dB.

POLARIZATION STABLE 795NM VCSELS

VCSELs, in general being radially symmetric, exhibit low dichroism or birefringence, and the lack of any polarization anisotropy in the modal gain leads to devices being inherently polarization unstable. This is a problem for VCSELs intended for atomic clocks, or any other application where polarization stability is of importance.

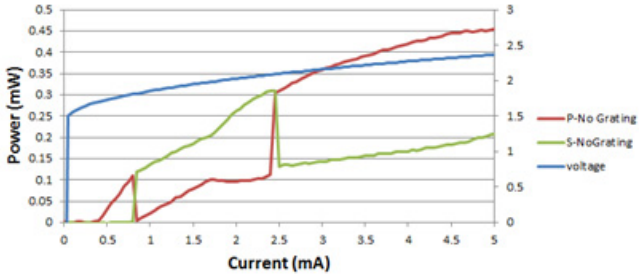

Figure 5 Example of polarization instability in a 795nm VCSEL.

Figure 5 shows an example of this instability, where the distribution of the optical power between two orthogonal polarization states can be observed to switch as a function of bias current, apparently at random. Such behavior is typical, and can be induced by a number of factors besides current, including mounting stress, ambient temperature fluctuations, and optical feedback.

What is desired is a device that is unconditionally stable, with the polarization well oriented along a preferred direction with respect to the die edge. In our case, this has been accomplished by etching shallow surface relief gratings approximately 40nm deep into the aperture region of the devices to increase the threshold gain of the polarization mode oriented along the grating direction to the point where it is effectively suppressed. (Fig. 6) The grating consists of 0.3um lines and spaces. What is important to note is that these gratings were patterned using optical as opposed to e-beam lithography, attractive for low cost manufacturing.

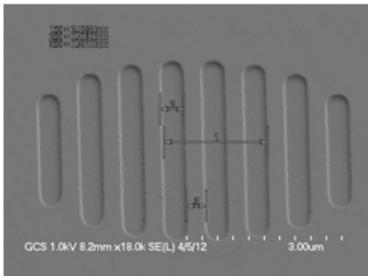

Figure 6 SEM image of a 40nm deep linear grating etched in the aperture region of a 795nm VCSEL to achieve polarization control.

TABLE I
POLARIZATION PERFORMANCE OF GRATING VCSELS

Grating Orientation	Probability of Polarization Switch	Avg Degree of Polarization
Horizontal	0.0%	-0.937
None	65.6%	-0.523
Vertical	0.46%	0.927

Table I shows the statistics from the measurement of ~75K lasers on a single 4" wafer, including devices with and without gratings. Gratings were oriented in both horizontal and vertical directions with respect to the wafer. Compared to devices without gratings, devices with gratings showed an extremely low probability of polarization switching, and a high degree of polarization (DOP) along the grating axes. (DOP = +1 or -1 for perfect vertical or horizontal polarization respectively)

1860NM VCSELS FOR NEURAL STIMULATION

The 1860nm VCSELs developed at Vixar are based on InP-compatible materials and incorporate highly strained InGaAs quantum wells. Challenges include the very thick epitaxy that must be grown because of the low index contrast available in materials for the DBRs. The mirrors must be comprised partially of quaternary materials, which leads to inherently poor thermal conductivity. Achieving good electron confinement in the active region is difficult due to the low conduction band offset, and non-radiative recombination is problematic since Auger processes become important as the quantum well bandgap decreases. Therefore low gain and poor temperature performance are critical issues.

The bottom-emitting device of Fig.7 uses a hybrid dielectric mirror design to achieve high reflectivity while minimizing the total semiconductor thickness. The bottom

DBR is all-epitaxial, while the top DBR consists of a partial semiconductor DBR followed by a deposited dielectric stack. An intra-cavity tunnel junction is included above the active region, allowing both DBRs to be doped n-type for lower loss and higher conductivity. Current confinement in the device is achieved by a two-step ion implantation process, resulting in a planar fabrication process with a single epitaxial growth step.

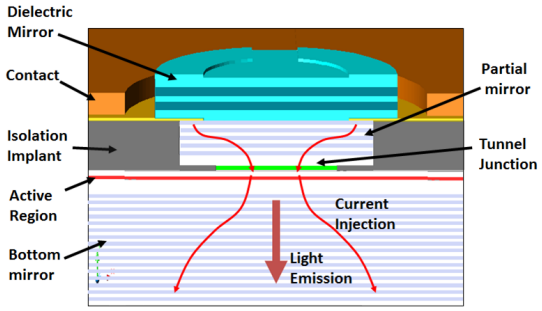

Figure 7 Schematic of hybrid dielectric mirror bottom-emitting 1860nm VCSEL structure.

Figure 8 shows the light versus current and voltage measured CW at room temperature. Lasing is observed for aperture sizes varying between 8 and 50µm. Threshold current densities are 1-2kA/cm2 and the lowest threshold current is 1.1 mA for the smallest device. The maximum CW power measured is 7.2 mW for a 50µm diameter device. To our knowledge this is the highest CW power reported for an 1860nm VCSEL. CW operation has been observed as high as 85°C. The peak wall plug efficiency was 9.5%.

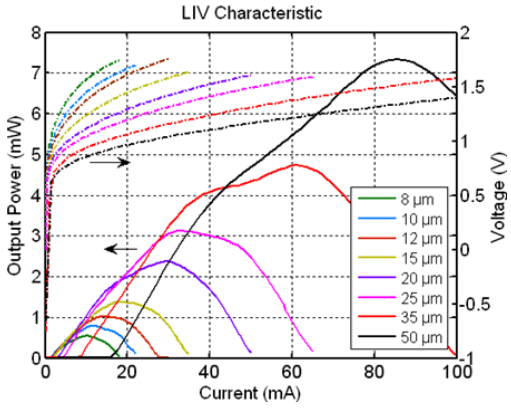

Figure 8 Room temperature CW performance of 1860nm VCSELs with various aperture diameters.

CONCLUSIONS

The many attractive attributes of vertical-cavity lasers make them suitable as optical sources in a broad range of areas outside of traditional 850nm fiber communications. The development has proven difficult due to the many materials and processing challenges, but significant progress has been made. 795nm VCSELs for atomic clocks and 680nm VCSELs for plastic optical fiber are now ready for commercialization. Current 1860nm devices show promise for infrared neuro-stimulation, and continued improvements on output power and efficiency will help to widen the scope of future applications.

ACKNOWLEDGEMENTS

The authors would like to thank TATRC and Mark Bendett at Lockheed Martin Aculight, as well as the NSF SBIR program for its support of this work.

REFERENCES

[1] Asai, Inuzuka, Koike, Takahashi and Koike, *J. Lightwave Technology* vol. 29, p. 1620, 2011.

[2] Y. Ohtsuka and Y. Hatanaka, "The preparation of light-focusing plastic fiber by heat-drawing process", *Applied Physics Letters*, vol. 29, no. 11, pp. 735-737, 1976.

[3] R. Nakao, A. Kondo, and Y. Koike, "Fabrication of High Glass Transition Temperature Graded-Index Plastic Optical Fiber: Part 2 – Fiber Fabrication and Characteristics", *J. Lightwave Technology*, vol. 30, no. 7, pp. 969-973, 2012.

[4] Ying-Ying Huang, et al., "Biphasic Response in Low Level Light Therapy", *Proc. International Dose-Response Society*, ISSN:1559-3258, Univ. of Mass., 2009.

[5] J.E. Sinex, "Pulse oximetry principals and limitations," *J Emerg Med* vol. 17, pp. 59-67, 1999.

[6] J. Kitching, et al., "A Microwave Frequency Reference Based on VCSEL-Driven Dark Line Resonances in Cs Vapor", *IEEE Trans. On Instrumentation and Measurement*, vol. 49, no. 6, pp. 1313-17, 2000.

[7] D. K. Serkland, et al., "VCSELs for Atomic Sensors", in *Vertical-Cavity Surface-Emitting Lasers XI*, Proc. of SPIE Vol. 6484, 2007.

[8] J. Wells, et al., "Optical stimulation of neural tissue in vivo," *Opt. Lett.* vol. 30, no. 5, pp. 504-507, 2005.

[9] A. Izzo, et al., "Optical parameter variability in laser nerve stimulation: a study of pulse duration, repetition rate, and wavelength," *IEEE Transactions on Biomedical Engineering*, vol. 54, no. 6, pp. 1108-1114, 2007.

[10] J.Walsh and J. Cummings, "Effect of the dynamic optical properties of water on midinfrared laser ablation," *Lasers in surgery and medicine*, vol. 15, no. 3, pp. 295-305, 1994.

[11] M. Hibbs-Brenner, K. Johnson, and M. Bendett, "VCSEL technology for medical diagnostics and therapeutics", in *Proc. SPIE*, 7180, pp. 71800-71810, 2009.

[12] J. A. Lott and R. P. Schneider, "Electrically injected visible (639–661 nm) vertical cavity surface emitting lasers," *Electronics Letters*, vol. 29, no. 10, pp. 830–832, 1993.

ACRONYMS

VCSEL: Vertical Cavity Surface Emitting Laser
POF: Plastic Optical Fiber
PMMA: Polymethyl Methacrylate
LED: Light Emitting Diode
INS: Infrared Neural Stimulation
SCH: Separate Confinement Heterostructure
MOCVD: Metal Organic Chemical Vapor Deposition
BCB: Benzo Cyclo Butene
CW: Continuous Wave
DBR: Distributed Bragg Reflector